Research Article

Xiaoyu Jie, Bing-Chiuan Shiu, Huazhong Wu, Yuchi Zhang, Yuansong Ye, Chunxiang Lin*, and Run Fang*

Adsorption and recovery of Cr(vI) from wastewater by Chitosan-Urushiol composite nanofiber membrane

https://doi.org/10.1515/epoly-2023-0157 received September 30, 2023; accepted December 07, 2023

Abstract: Chitosan (CS) is widely used in the treatment of wastewater containing metal ions. However, the poor stability in acidic aqueous solutions severely limits its application in many practical scenarios. In this work, a CS-based composite nanofiber membrane was prepared by electrospinning using urushiol, a natural biomaterial, as the cross-linking agent. The application of the CS-urushiol (CS-U) membrane in the adsorption and recovery of Cr(vi) in wastewater was systematically studied. The CS-U membrane showed great resistance to strongly acidic and oxidative environments, and the adsorption process combined two mechanisms of electrostatic attraction and redox reaction. Due to the nanoscale fibers, porous structure, and strong acid resistance, the CS-U membrane adsorbed Cr(v1) rapidly and efficiently in both batch and continuous modes. Moreover, the adsorption capacity and selectivity of the CS-U membrane for Cr(v1) could be maximized simultaneously by adjusting the solution pH, promoting the recovery of high-purity Cr₂O₃.

Bing-Chiuan Shiu, Yuchi Zhang, Yuansong Ye: College of Material and Chemical Engineering, Minjiang University, Fuzhou 350108, China; Fujian Engineering Research Center of New Chinese Lacquer Materials, Fuzhou 350108. China

Huazhong Wu: College of Material and Chemical Engineering, Minjiang University, Fuzhou 350108, China

Keywords: chitosan, urushiol, nanofiber membrane, Cr(v_I) adsorption, biosorbent

1 Introduction

Cr(vi) contained in industrial wastewater, especially electroplating wastewater, is a highly toxic pollutant. It can enter the body through skin contact, ingestion, and inhalation, causing varying degrees of damage (1-3). In severe cases, Cr(vi) can even cause genetic mutations, cancer, and infantile deformities. Therefore, the World Health Organization classifies Cr(vi) as a Group 1 carcinogen. At present, Cr(vi)-containing industrial wastewater is commonly treated by the reduction-precipitation method, i.e., reduction of Cr(vi) to Cr(iii) using a reducing agent followed by precipitation and removal of Cr(III) by adjusting the solution pH (4,5). However, industrial wastewater often contains many kinds of metal ions simultaneously. The application of the reduction-precipitation method results in the formation of large quantities of mixed sludge containing a variety of metal hydroxides, which is extremely difficult to treat. Thus, in recent years, various environmentally friendly methods have been developed for treating Cr(vi)-containing wastewater, such as ion exchange (6,7), membrane separation (8-10), and adsorption (11-13). Among these methods, adsorption has the distinctive advantages, including ease of operation, wide applicability, and minimal secondary pollution. This makes it particularly suitable for the deep treatment of low-concentration Cr(v1)-containing wastewater. In view of the strongly acidic and oxidative characteristics of Cr(vi)-containing wastewater, finding an adsorbent that is simultaneously environmentally friendly, highly adsorptive, and structurally stable is a key factor in enhancing the adsorption efficiency of Cr(vi).

Chitosan (CS) is produced by deacetylating chitin, which is a renewable and environmentally friendly natural polymer. Under acidic conditions, the amine groups on CS can be

^{*} Corresponding author: Chunxiang Lin, College of Environment and Safety Engineering, Fuzhou University, Fuzhou 350108, China, e-mail: lcx2010@fzu.edu.cn

^{*} Corresponding author: Run Fang, College of Material and Chemical Engineering, Minjiang University, Fuzhou 350108, China; College of Environment and Safety Engineering, Fuzhou University, Fuzhou 350108, China; Fujian Engineering Research Center of New Chinese Lacquer Materials, Fuzhou 350108, China, e-mail: fangrun@mju.edu.cn
Xiaoyu Jie: College of Environment and Safety Engineering, Fuzhou University, Fuzhou 350108, China

protonated by H⁺ in water to form -NH₃⁺, which adsorbs anionic pollutants in water through electrostatic interactions. Since $Cr(v_1)$ mainly exists as anions of $HCr_2O_7^-$ and $Cr_2O_7^{2-}$ in acidic aqueous solution (9,11), CS can effectively adsorb Cr(vi) from wastewater through electrostatic adsorption. Compared with powdered and bulk CS, the specific surface area of CS nanofiber membrane prepared by electrospinning is significantly enhanced, which substantially improves the adsorption rate and adsorption capacity of the adsorbent. However, the huge specific surface area reduces the stability of the membrane in acidic solutions and makes it vulnerable to breakage and dissolution. To address this issue, cross-linking agents such as glutaraldehyde (C₅H₈O₂) (14,15) and epichlorohydrin (16,17) are often used to transform linear CS molecules into a cross-linked network. Although such modifications are effective in enhancing the acid resistance of CS nanofiber membrane, most of these chemical cross-linkers are non-renewable and cytotoxic.

Lacquer is a natural polymer paint harvested from the lacquer tree, and urushiol is its major component and filmforming substance. The paint film formed by the curing urushiol has excellent resistance to abrasion, acids, and solvents. Urushiol is derived from catechol with long side chains having varying degrees of unsaturation. The adjacent phenolic hydroxyl groups offer reactive sites and reducing properties for urushiol, and the long unsaturated side chains are the primary origin of hydrophobicity. Due to the high reactivity of the catechol group and the unsaturated alkyl chain, urushiol can easily stick to the surfaces of various polymeric (18), inorganic, and metallic materials by forming chemical bonds with them (19,20). Based on these properties, we expect that urushiol can be used to cross-link CS instead of non-renewable chemical crosslinking agents for the preparation of a CS-urushiol (CS-U) composite nanofiber membrane, which may enhance the acid resistance of the nanofiber membrane in a more environmentally friendly way, and simultaneously achieve its rapid and high-capacity adsorption of Cr(vi) in water.

In this study, the CS-U nanofiber membrane was prepared by electrospinning and used to adsorb Cr(vi) in simulated wastewater. The adsorption mechanism was explored through a comprehensive characterization of the CS-U membranes before and after adsorption. To evaluate the crosslinking effect of urushiol, acid resistance tests were performed to investigate the stability of the membranes in acidic aqueous solutions. Batch adsorption experiments were conducted to reveal the effects of solution pH, adsorption time, Cr(vi) concentration, and coexisting ions on the adsorption behavior of the membranes. Moreover, the selective adsorption and the recovery of Cr(vi) in the presence of multiple metal ions were also investigated. Finally, continuous

adsorption experiments were performed to verify the potential application prospect of CS-U nanofiber membranes.

2 Materials and methods

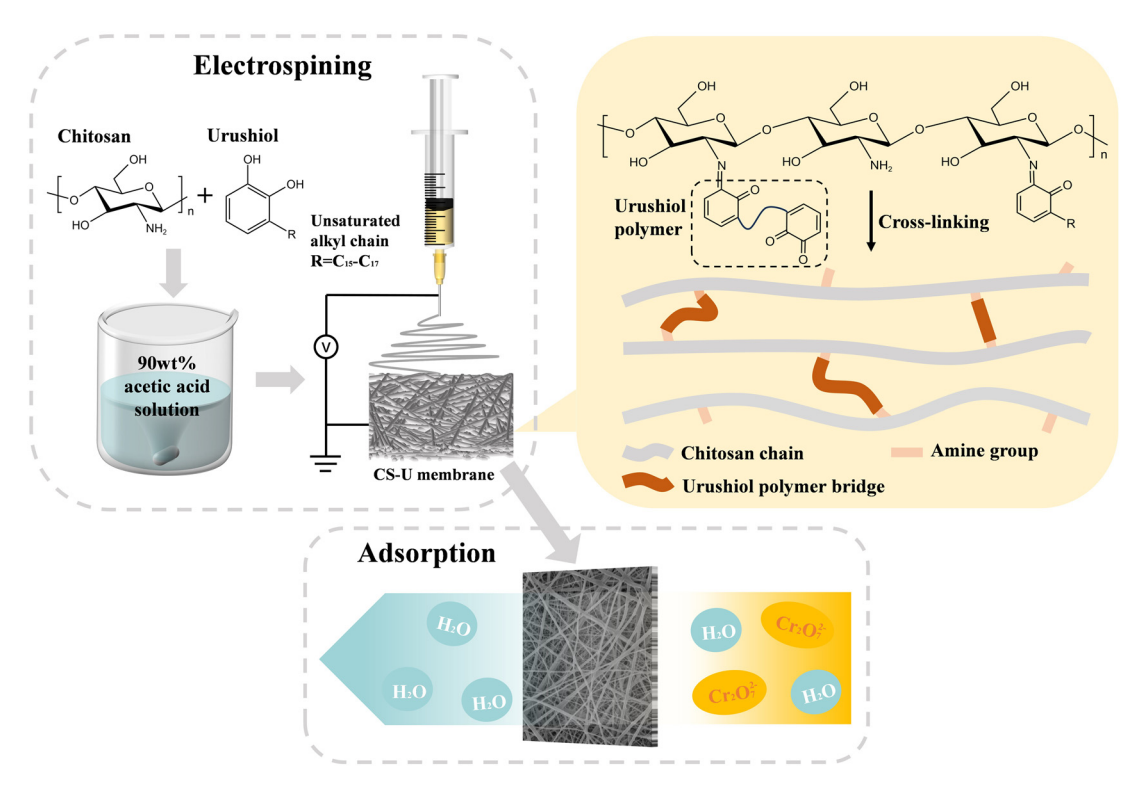
2.1 Materials

CS (DD = 90%, $M_{\rm w}$ = 200 kDa) was purchased from Macklin Biochemical Technology Co, Ltd. (Shanghai, China). Polyethylene oxide (PEO, 100 kDa), $C_5H_8O_2$ (50 wt% in aqueous solution), acetic acid (CH₃COOH), potassium dichromate (K₂Cr₂O₇), sodium chloride (NaCl), sodium sulfate (Na₂SO₄), potassium nitrate (KNO₃), zinc chloride (ZnCl₂), copper chloride dihydrate (CuCl₂·2H₂O), nickel nitrate hexahydrate (Ni(NO₃)₂·6H₂O), and diphenyl carbamide (C₁₃H₁₄N₄O) were of analytical or biochemical reagent grade and purchased from Aladdin Industrial Co., Ltd. (Shanghai, China). Urushiol, a brown viscous liquid, was extracted from natural raw lacquer produced in Shanxi, China, according to the method described in the literature (21).

2.2 Preparation of CS-U and CS-GA nanofiber membranes

The preparation of the CS-U nanofiber membrane was divided into two steps as shown in Scheme 1: preparation of spinning solution and electrospinning. During the preparation of the spinning solution, 1.0 g of CS and 0.2 g of PEO were first added to a mix solution containing 27.0 g of CH₃COOH and 3.0 g of deionized water, followed by stirring at room temperature for 8 h to completely dissolve the solute. Then, 0.2 g of urushiol was added and stirring was continued for 2 h. The well-mixed solution was left to stand for 1 h to obtain the spinning solution. The second step was the preparation of the CS-U nanofiber membrane by electrospinning machine with the following conditions: spinning voltage of 23 kV, injection rate of 1.0 mL·h⁻¹, receiving distance of 15 cm, humidity of 35%, and receiving medium was aluminum foil. After electrospinning, the obtained nanofiber membrane was air-dried at 60°C to remove residual solvent.

The CS-GA nanofiber membrane was used as the control sample. A beaker containing the neat CS nanofiber membrane was placed in a desiccator containing 20 mL of $C_5H_8O_2$ (50 wt%). Then, the CS membrane was crosslinked with $C_5H_8O_2$ vapor for 24 h. At the end of crosslinking, the CS-GA nanofiber membrane was air-dried to remove the residual cross-linking agent.



Scheme 1: Schematic illustration of the preparation and application of the CS-U composite nanofiber membrane.

2.3 Characterization of the nanofiber membranes and acid resistance tests

The morphology of the CS-U nanofiber membrane was observed using a scanning electron microscope (SU8010, Hitachi, Japan). The specific surface area of the membrane was measured by the Brunauer-Emmett-Teller (BET) method using an ASAP2020 adsorption analyzer (Micromeritics, U.S.). The chemical structure of the membrane, before and after adsorption, was analyzed by a fourier transform infrared (FT-IR) spectrometer (iS50, Thermo Nicolet, U.S.) and a K-alpha X-ray photoelectron spectroscopy (XPS) (Thermo Scientific, U.S.). In acid resistance tests, the neat CS membrane without cross-linking (CS-BLK) was used as the blank control. Rectangular samples of CS-BLK, CS-GA, and CS-U membranes were placed in a $K_2Cr_2O_7$ solution at pH = 3. After soaking for different periods of time, changes in the appearance of the membranes were compared.

2.4 Batch adsorption experiments

To evaluate the adsorption capacity of the CS-U nanofiber membrane, batch adsorption experiments were carried out in a constant temperature water bath shaker using $K_2Cr_2O_7$ solution as simulated wastewater. The effects of

solution pH, initial Cr(vi) concentration, and coexisting ions on the adsorption performance of the CS-U membrane were investigated. With diphenyl carbazide being the chromogenic agent, a UV-vis spectrophotometer (UV-2450, Shimadzu, Japan) was used to record the absorbance of the solution at 540 nm and the Cr(vi) concentration was calculated accordingly. The adsorption capacity $q_{\rm e}$ (mg·g⁻¹) of CS-U and CS-GA membranes was calculated in the following equation:

$$q_e = \frac{(C_0 - C_e) \times V}{m} \tag{1}$$

where C_e and C_0 (mg·L⁻¹) are the equilibrium and initial concentrations of Cr(v_I), respectively, q_e (mg·g⁻¹) is the equilibrium adsorption capacity, V(L) is the volume of solution, and m (g) is the adsorbent dose.

To investigate the effect of pH on the adsorption capability of the nanofiber membranes, 50 mL of $K_2Cr_2O_7$ solution with a concentration of $50 \text{ mg} \cdot \text{L}^{-1}$ was used as a simulated wastewater. The solution pH was adjusted to 2–7 followed by the addition of 10 mg of adsorbent. To study the adsorption kinetics, the solution pH was set to 3. About 10 mg of the membrane was added, and the adsorption capacity was determined after different adsorption time. To study the effect of initial $Cr(v_1)$ concentration on the adsorption, 10 mg of the membrane was added to 50 mL of $K_2Cr_2O_7$ solutions at pH = 3 with different initial $Cr(v_1)$ concentrations.

2.5 Interference of coexisting ions and selective adsorption

To investigate the influence of coexisting ions on the adsorption capacity of the CS-U membrane, batch experiments were conducted by adding the anions (Cl⁻, SO₄²⁻, and NO₃⁻) and cations (Cu²⁺, Zn²⁺, and Ni²⁺), which were typically found in Cr(vi)-containing wastewater, into the K₂Cr₂O₇ solutions. Each coexisting ion had a concentration of 50 mg·L⁻¹, consistent with the concentration of Cr(v_I), and the pH of the solution was adjusted to 3. After 8 h of adsorption, the residual concentration of Cr(vI) was measured and the adsorption amount of the CS-U membrane was calculated. The selective adsorption of Cr(vi) by the CS-U membrane was also investigated. The CS-U membrane was added to the simulated wastewater containing $Cr_2O_7^{2-}$, Cu²⁺, Zn²⁺, and Ni²⁺. The concentration of each metal ion was 50 mg·L⁻¹, and the solution pH was adjusted to 2-5. After 8h of adsorption, the concentration of each ion remained in the mixed solution was measured by an inductively coupled plasma-optical emission spectroscopy (ICP-OES) (720, Agilent, USA), from which the amount of each ion adsorbed by the CS-U membrane was compared.

2.6 Continuous adsorption

In the continuous adsorption experiments, a peristaltic pump was used to transport $K_2Cr_2O_7$ solution (10 mg·L⁻¹, pH = 3) bottom-up into an adsorption column filled with the CS-U nanofiber membranes at a flow rate of $4 \,\mathrm{mL \cdot min}^{-1}$. The concentration of Cr(vi) in the effluent was measured periodically to obtain the dynamic adsorption curve. The doses of the adsorbent used for the three continuous adsorption experiments were 120, 160, and 200 mg, respectively. The breakthrough and saturation points were defined as the time when the effluent concentration reached 5% and 95% of the influent concentration, respectively. The exhaustive adsorption amount at saturation, $q_{\rm exh}$ (mg·g⁻¹), was calculated according to the following equations:

$$q_{\text{total}} = \frac{vA}{1,000} = \frac{v}{1,000} \int_{0}^{t} (C_0 - C_t) dt$$
 (2)

$$q_{\rm exh} = \frac{q_{\rm total}}{m} \tag{3}$$

where $q_{\rm total}$ (mg) is the total mass of Cr(v_I) adsorbed by CS-U nanofiber membrane in the adsorption column, v (mL·min⁻¹) is the flow rate, C_0 and C_t (mg·L⁻¹) are the Cr(v_I) concentrations in the influent and effluent, respectively, and t (min) is the adsorption time.

3 Results and discussion

3.1 Characterization of CS-U composite nanofiber membrane

It has been demonstrated in our previous research work that CS and urushiol can form a unique cross-linked structure with hydrophilic CS molecules as the backbone and hydrophobic urushiol polymers as the cross-linking bridges (Scheme 1). This is achieved by means of Schiff base reaction between the amine groups on CS and the catechol groups on urushiol (22). The FT-IR spectra of CS-GA and CS-U are shown in Figure 1a. The characteristic peak at 1,588 cm⁻¹ belonged to the bending vibration of -NH₂, and the numerous amine groups led to the excellent adsorption capacity of CS for Cr(vi). With the addition of urushiol, the FT-IR spectrum of CS-U showed a characteristic peak of phenolic hydroxyl at 1,280 cm⁻¹, and the stretching vibration of methylene group at 2,918 cm⁻¹ was significantly enhanced, which came from the catechol groups and alkyl side chains of urushiol, respectively. These changes suggested that the addition of urushiol not only promoted the cross-linking of CS nanofibers but also provided the composite nanofiber membrane with a number of reducing catechol groups and hydrophobic alkyl chains. As shown in Figure 1b and c, the contact angles of the CS-GA and CS-U membranes were 61.2° and 80.3°, respectively, verifying the enhancement of the hydrophobicity of the membrane after the modification of urushiol.

By comparing the FT-IR spectra of CS-U before and after adsorption in Figure 1a, it can be found that the peaks in the region of 1,580–1,640 cm⁻¹ appeared to be significantly broadened. This may be attributed to the participation of amine groups in the adsorption of Cr(vi). Similar phenomenon has been reported in the studies on CS adsorption (23,24). In acidic K₂Cr₂O₇ solution, the protonated amine groups were positively charged and then adsorbed the negatively charged Cr₂O₇²⁻ and HCr₂O₇⁻ ions by electrostatic interaction, resulting in the changes in the intensity and position of the amine peaks. Moreover, the broadening of the characteristic peak could also be caused by the oxidation of the catechol groups, resulting in the formation of carbonyl groups. This speculation can be verified by the disappearance of the characteristic peak of phenolic hydroxyl group at 1,280 cm⁻¹. After adsorption, two new peaks were observed at 780 and 890 cm⁻¹, which were attributed to Cr(III)-O and Cr(VI)-O, respectively. This suggested that the CS-U membrane adsorbed a large amount of Cr(vi) and partially converted it to Cr(iii). From the aforementioned analysis, it can be seen that the addition of urushiol endowed the CS-U membrane with a certain degree of hydrophobicity and reducibility, and the

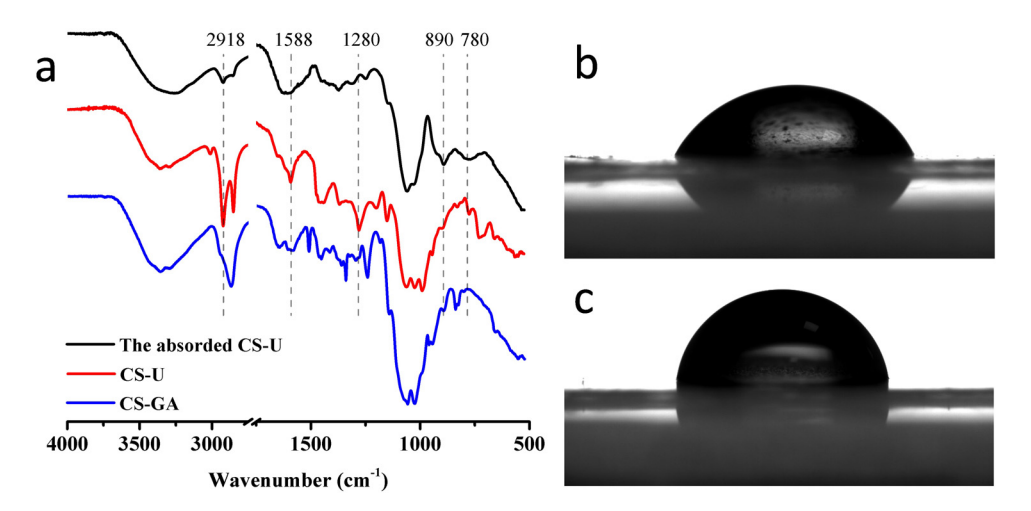


Figure 1: (a) FT-IR spectra of the CS-GA, CS-U, and adsorbed CS-U membranes and (b, c) water contact angles of the CS-GA and the CS-U nanofiber membranes, respectively.

adsorption of Cr(vi) may involve two mechanisms, namely, electrostatic adsorption and redox reaction.

In addition to being able to qualitatively analyze elemental compositions and atomic valence states, XPS is able to obtain information on the relative content of elements through peak area calculations. The XPS spectra of CS-GA and CS-U membranes after the adsorption of Cr(vi) are presented in Figure 2a and b, respectively. The Cr2p peaks, observed in both figures, indicated that both membranes were capable of efficiently adsorbing Cr(vi) in wastewater. Figure 2c and d shows the Cr2p spectra of the membranes after Cr(vi) adsorption. The peaks at 576.1 and 585.5 eV belonged to Cr(III), and the peaks at 578.3 and 587.4 eV belonged to Cr(vi). By integrating the peak areas, the ratios of Cr(III) to Cr(VI) on the surface of CS-U and CS-GA membranes were calculated to be 2.3:1 and 1.6:1, respectively. The higher ratio of Cr(III) to Cr(VI) suggested that the appearance of urushiol promoted the redox reaction, resulting in the reduction of more Cr(vI) to Cr(III).

Figure 2e and f shows the C1s spectra of the CS-U membrane before and after $Cr(v_I)$ adsorption, respectively. Four characteristic peaks can be seen in both figures, belonging to C-C/C-H (284.8 eV), C-N (286.1 eV), C-O (286.5 eV), and C=O (288.3 eV). By comparing Figure 2e and f, it can be found that the content of C-C decreased after $Cr(v_I)$ adsorption, while the content of C-O and C=O increased significantly, confirming that the CS-U membrane was oxidized after prolonged contact with acidic $K_2Cr_2O_7$ solution. Furthermore, the ratio of C=O to C-O increased from 0.37 to 0.43 after $Cr(v_I)$ adsorption, which might be caused by the oxidation of the catechol groups of urushiol to quinone compounds. This is consistent with the variations in the FT-IR spectra of the CS-U membrane before and after $Cr(v_I)$ adsorption.

From the FT-IR and XPS analyses, it can be seen that the removal of Cr(v1) by CS-U membrane combined the two mechanisms of electrostatic adsorption and redox reaction, which not only ensured the high adsorption capacity of the composite nanofiber membrane, but also converted Cr(v1) to the much less toxic Cr(III).

The SEM image in Figure 3a shows the microscopic morphology of the CS-U membrane. The composite nanofiber membrane was composed of numerous nanofibers that were woven in a random manner, creating many pores among the fibers. Porous structure resulted in a large specific surface area and facilitated its rapid adsorption of pollutants. Despite the significant molecular structure and solubility differences between urushiol and CS, the CS-U membrane had a smooth surface without apparent phase separation. Combined with the FT-IR and XPS analyses, it can be inferred that the Schiff base reaction between urushiol and CS produced a homogeneous copolymer. Meanwhile, as can be seen in Figure 3b, the fiber diameters of CS-U membrane were dominantly in the range of 0-400 nm, and the number of fibers with diameters less than 200 nm exceeded 80%. The nanoscale fibers and the porous structure provide the CS-U membrane with a huge BET surface area of 7.36 m²·g⁻¹, which is nearly 100 times larger than that of powdered CS with a typical BET surface area of 0.05-0.1 m²·g⁻¹, leading to a high adsorption rate and a large adsorption capacity (16).

3.2 Acid resistance test

Cr(vi)-containing wastewater is commonly acidic and oxidizing, whereas CS is readily soluble in acidic aqueous solutions due to the existence of amine groups. Therefore, when used for the adsorption of Cr(vi), CS usually needs to

6 — Xiaoyu Jie et al. DE GRUYTER

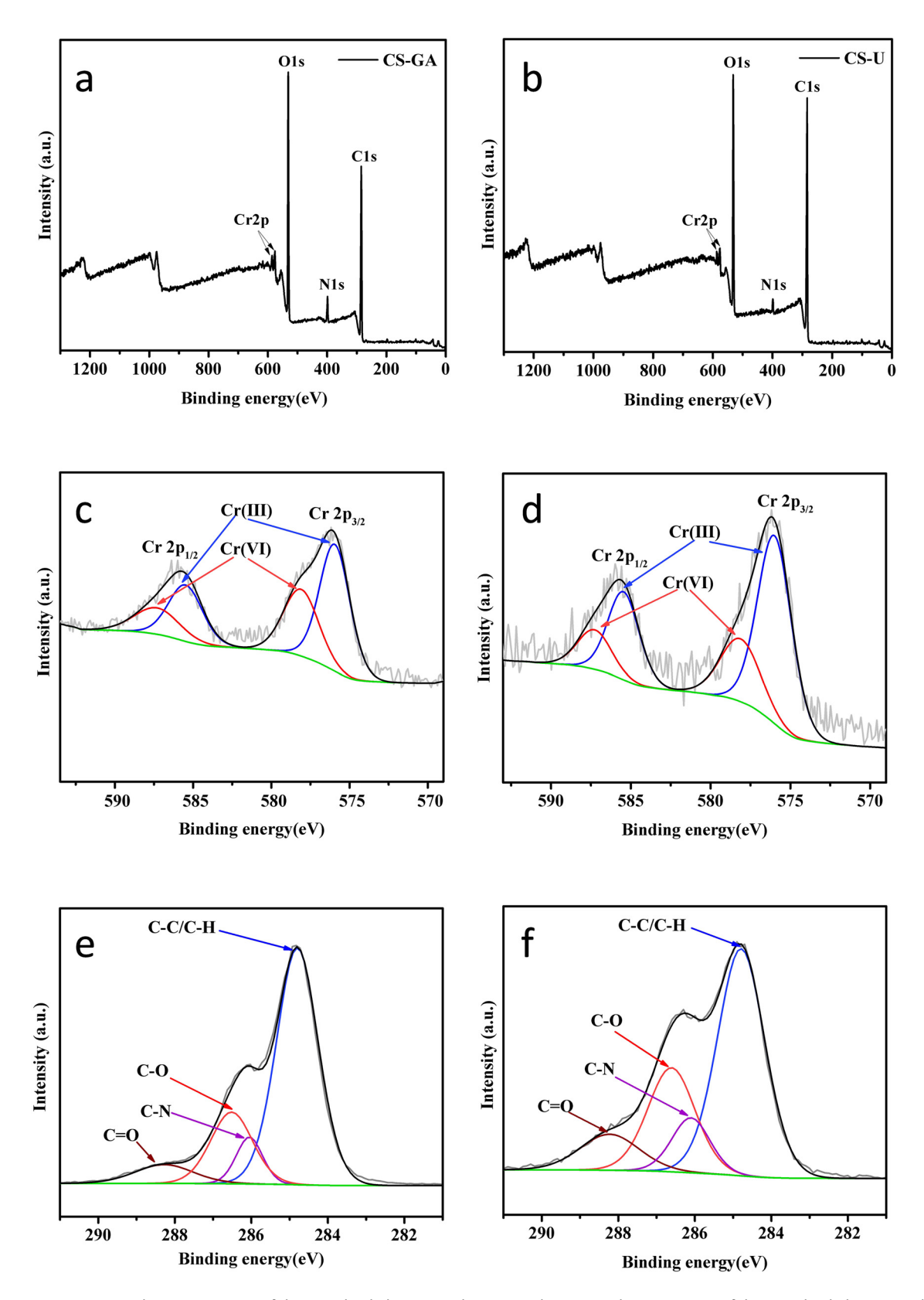


Figure 2: XPS spectra, (a, b) survey spectra of the Cr(v_I)-loaded CS-GA and CS-U membranes, (c, d) Cr2p spectra of the Cr(v_I)-loaded CS-GA and CS-U membranes, and (e, f) C1s spectra of the CS-U membrane before and after adsorption.

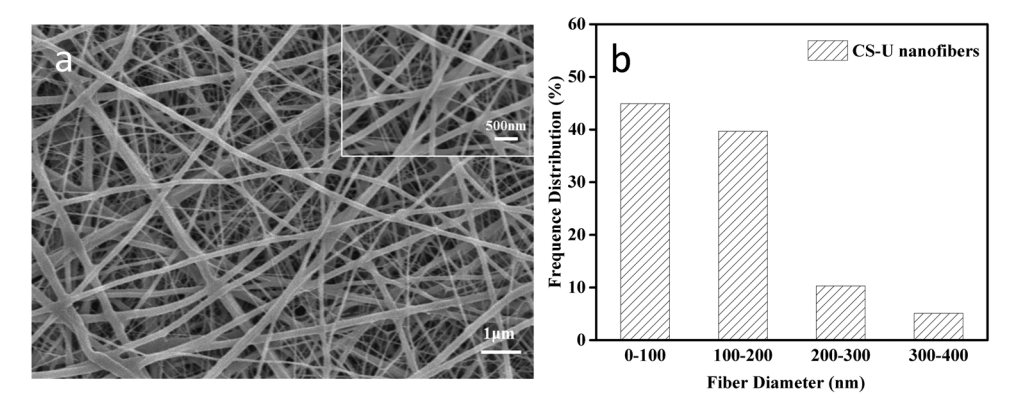


Figure 3: Microscopic morphology of the CS-U nanofiber membrane: (a) SEM image of the CS-U membrane and (b) diameter distribution of the CS-U nanofibers.

undergo a cross-linking reaction to transform from a linear polymer to a more stable network polymer. C₅H₈O₂ is the most widely used cross-linking agent due to its high reactivity and good cross-linking effect. The acid resistance of three nanofiber membranes, namely, CS-BLK, CS-GA, and CS-U, in a $K_2Cr_2O_7$ solution with pH = 3 and C_0 = 50 mg·L⁻¹ is shown in Figure 4. Uncross-linked CS-BLK membrane was rapidly fragmented and then gradually dissolved in the solution after 4 h of shaking. Although C₅H₈O₂ cross-linking made the CS-GA membrane more acid-resistant, it began to fragment after 8 h of shaking and partially dissolved after 24 h. In contrast, the CS-U membrane exhibited excellent acid resistance. Even after 24 h of prolonged shaking, the CS-U membrane kept its appearance intact and did not dissolve at all. Cured urushiol has been proven to have excellent acid and corrosion resistance (25,26). As a result, the network structure formed by the cross-linking of urushiol endowed the CS-U membrane with excellent acid resistance

and structure stability in acidic K₂Cr₂O₇ solutions compared to traditional C₅H₈O₂.

3.3 Batch adsorption study

3.3.1 Effect of pH

The adsorption capacity of CS is strongly influenced by the pH of the solution. This is due to the effect of solution pH on both the type of metal ion in the solution and the functional groups on the adsorbent surface. Under acidic conditions, Cr(vi) mainly exists in the form of HCr₂O₇ and $Cr_2O_7^{2-}$, which can be adsorbed by the protonated amine groups carried by CS through electrostatic attraction. According to Figure 5, the CS-GA and CS-U membranes exhibited increased adsorption capacities for Cr(vi) with

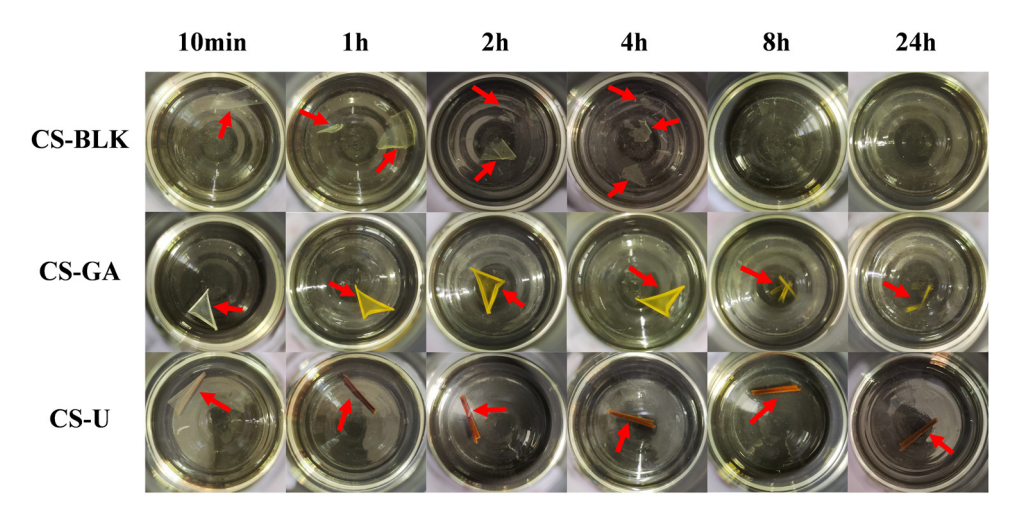


Figure 4: Appearance changes of three CS-based nanofiber membranes, CS-BLK, CS-GA, and CS-U, in K2Cr2O7 solution (experimental conditions: $C_0 = 50 \text{ mg} \cdot \text{L}^{-1}$, $T = 25^{\circ}\text{C}$, pH = 3).

8 — Xiaoyu Jie et al. DE GRUYTER

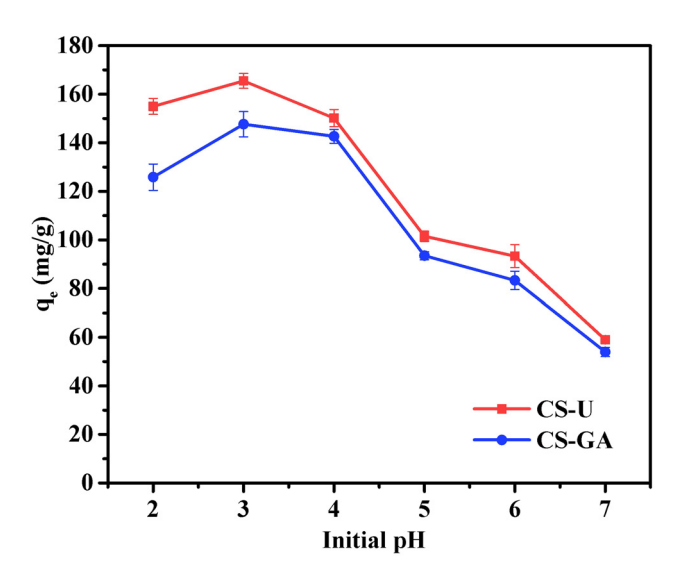


Figure 5: Effect of solution pH on the adsorption capacity of the CS-U and CS-GA membranes (experimental conditions: m = 10 mg, $C_0 = 50$ mg·L⁻¹, V = 50 mL, T = 25°C).

decreasing solution pH, as the strongly acidic environment promoted the protonation of amine groups, thus providing more positively charged adsorption sites. However, when the pH was further decreased to 2, $Cr(v_I)$ in the solution gradually transformed from $HCr_2O_7^-$ and $Cr_2O_7^{2-}$ to H_2CrO_4 (27–29), and the adsorption capacity of the membranes reduced accordingly. As a result, the adsorption capacity of both membranes for $Cr(v_I)$ reached its maximum in a strongly acidic environment at pH = 2-3, but this environment also significantly increased the solubility of CS (30). Benefiting from the unique cross-linking structure, the CS-U membrane had extremely strong acid resistance, which enabled it to adsorb $Cr(v_I)$ very efficiently in the strongly

acidic environment. It can also be found in Figure 5 that the adsorption capacity of CS-U was higher than that of CS-GA at each pH, especially at pH lower than 4. This suggested that the adsorption mechanism of CS-U was somewhat different from that of CS-GA, i.e., the addition of urushiol caused more redox reactions, which consequently improved the removal efficiency of Cr(vi).

3.3.2 Adsorption kinetics

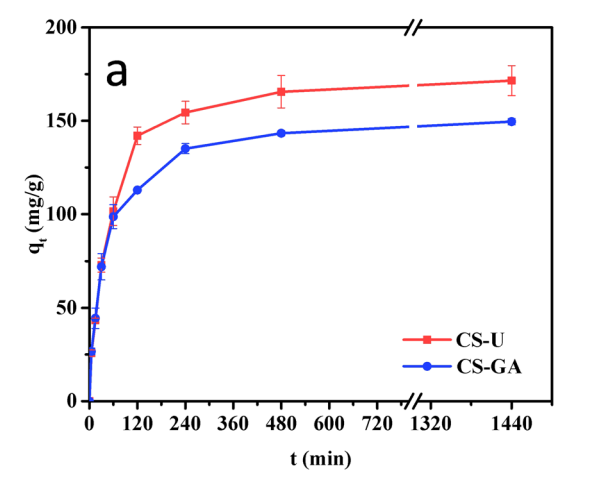
The nanoscale fibers and porous structure provided huge specific surface area and a large number of adsorption sites for the CS-U membrane, so that its adsorption rate is much higher than that of the traditional block or granular CS-based adsorbents. The adsorption behaviors of the CS-U and CS-GA membranes are shown in Figure 6. The adsorption amount of CS-U reached 72.89 and 142.01 mg·g⁻¹ after 30 min and 2 h adsorption, respectively, demonstrating a very high adsorption rate. As Eqs. 4 and 5, the pseudo-first-order model and the pseudo-second-order model were used to investigate the adsorption kinetics of the membranes:

$$q_t = q_e (1 - e^{-_1 k_t}) (4)$$

$$q_t = \frac{q_e^2 k_2 t}{1 + q_e k_2 t} \tag{5}$$

where k_1 and k_2 are the rate constants and q_t (mg·g⁻¹) is the adsorption amount at time t (s).

The fitting results are shown in Figure 6b, and the kinetic parameters are listed in Table 1. It can be seen that the pseudo-second-order kinetic model provided a better fit to the experimental data of the two membranes.



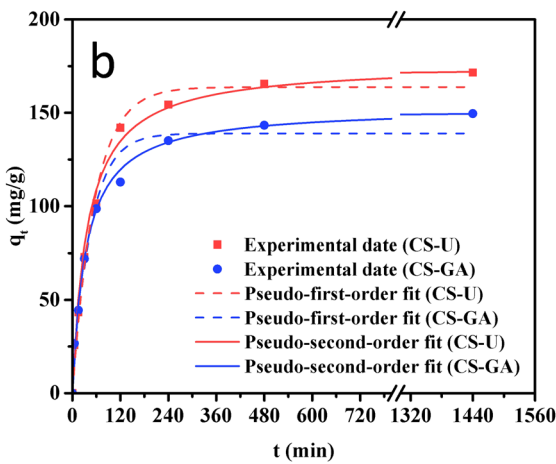


Figure 6: Adsorption kinetics of $Cr(v_1)$ by the CS-U and CS-GA membranes: (a) time profile and (b) fitting curves of pseudo-first-order model and pseudo-second-order models (experimental conditions: m = 10 mg, $C_0 = 50 \text{ mg} \cdot \text{L}^{-1}$, V = 50 mL, $T = 25^{\circ}\text{C}$, pH = 3).

Table 1: Kinetic parameters	for the adsorption of	Cr(vi) by the CS-U ar	d CS-GA membranes
-----------------------------	-----------------------	-----------------------	-------------------

Sample	q_e (exp) (mg·g $^{-1}$)	Pseudo-first-order model			Pseudo-second-order model		
		k ₁	q_e (cal) (mg·g $^{-1}$)	R ²	k ₂	q_e (cal) (mg·g $^{-1}$)	R ²
CS-U CS-GA	171.56 149.56	1.79×10^{-2} 2.10×10^{-2}	163.80 138.93	0.990 0.974	1.53×10^{-4} 1.96×10^{-4}	176.37 152.91	0.999 0.999

Moreover, the calculated value of the theoretical adsorption amount, $q_e(cal)$, was very close to the experimental value, $q_e(\exp)$, indicating that the adsorption of $Cr(v_1)$ involved a chemical adsorption process. It is worth mentioning that the adsorption amounts of Cr(vi) by CS-U and CS-GA were similar within 30 min. Subsequently, as the adsorption time increased, the adsorption amount of the CS-U membrane gradually exceeded that of CS-GA until the adsorption equilibrium was reached. This may be due to the fact that the combination of CS with urushiol changed the adsorption process from being dominated by electrostatic adsorption to a joint action of electrostatic adsorption and redox reaction. The initial stage of adsorption was mainly dominated by electrostatic adsorption, so the adsorption rates of CS-U and CS-GA were not significantly different. With the increase of adsorption time, urushiol on the CS-U membrane began to undergo redox reaction with Cr(vi), which led to the increase of the adsorption capacity of the CS-U membrane in the latter half of the adsorption process.

3.3.3 Adsorption isotherms

The effect of initial Cr(vi) concentration on the adsorption capacity of CS-U membranes was investigated, and the experimental data were fitted by Langmuir and Freundlich models in the following equations:

$$q_e = \frac{K_L q_{\text{max}} C_e}{1 + K_L C_e} \tag{6}$$

$$q_o = K_{\rm F} C_e^{\frac{1}{n}} \tag{7}$$

where $q_{\rm max}$ (mg·g⁻¹) is the maximum adsorption capacity, $K_{\rm L}$ and $K_{\rm F}$ are the equilibrium constants, and n is an empirical parameter for the Freundlich model. The fitting results and the isothermal parameters are shown in Figure 7 and Table 2.

As can be seen in Figure 7, the adsorption capacity of the CS-U membrane exceeded $200\,\mathrm{mg}\cdot\mathrm{g}^{-1}$ within the temperature range of 25–45°C. Such a high adsorption capacity was attributed to three factors: the excellent acid resistance

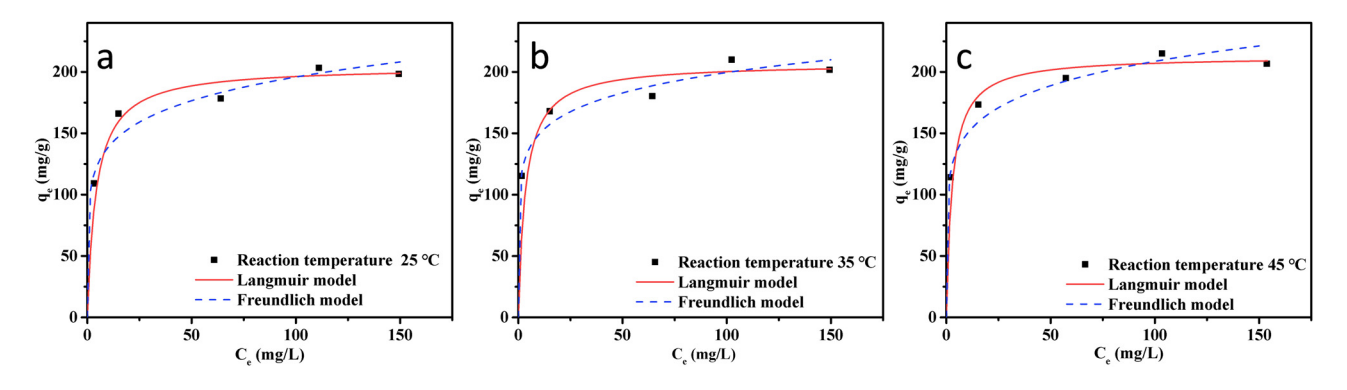


Figure 7: Fitting curves of the Langmuir and Freundlich models for $Cr(v_1)$ adsorption on the CS-U membrane at (a) 25°C, (b) 35°C, and (c) 45°C (experimental conditions: m = 10 mg, V = 50 mL, pH = 3).

Table 2: Isotherm parameters for the Cr(vI) adsorption by the CS-U membranes

Temperature (°C)	ı	angmuir model			Freundlich model	el
	q _{max} (mg·g ⁻¹)	KL	R ²	K _F	n	R ²
25	204.50	4.89×10^{-3}	0.997	98.24	6.68	0.912
35	207.04	4.83×10^{-3}	0.996	111.90	7.96	0.951
45	212.77	4.70×10^{-3}	0.998	107.48	6.94	0.940

Table 3: Maximum adsorption capacity of different adsorbents for Cr(vI)

Adsorbents	q _{max} (mg·g ^{−1})	рН	References
Polyethyleneimine-cross-linked graphene oxide	436.20	2	(11)
Zn-MOF/CS (ZnBDC/CSC) composite	225.00	5	(31)
Composite CS biosorbent	158.85	4	(32)
CS-grafted graphene oxide nanocomposite	104.16	2	(23)
CS/PMMA composite nanofiber membranes	94.80	2	(33)
CS-based hydrogel	93.03	4.5	(34)
Magnetic cyclodextrin-CS/graphene oxide	67.66	3	(35)
Ethylenediamine-modified cross-linked magnetic CS resin	51.81	2	(13)
CS-U nanofiber membrane	204.50	3	This work

enabled the CS-U membrane to adsorb Cr(vI) effectively in strongly acidic solutions, the nanoscale fibers and porous structure brought the active adsorption sites on the membrane into full contact with Cr(vI), and the addition of urushiol converted more Cr(vI) to Cr(III). The Langmuir model provided a better fit to the experimental data than the Freundlich model, suggesting that it was a monolayer adsorption on the uniformly distributed adsorption sites. This is consistent with the adsorption behavior of many CS-based adsorbents. Table 3 compares the maximum adsorption capacity of several novel adsorbents for Cr(vI), such as GO/CS composites, MOFs, nanofiber membranes, and nanoparticles, under similar adsorption conditions. It is evident that the CS-U membrane has higher adsorption capacity than the most CS-based adsorbents.

3.3.4 Interference of coexisting ions

Industrial wastewater often contains various types of anions and cations. When the protonated amine groups on CS adsorb Cr(vi) through electrostatic attraction, anions in the wastewater may compete with Cr(vi) for adsorption sites. Meanwhile, some metal ions may chelate with the amine groups and thus occupy specific adsorption sites (36). To evaluate the effect of coexisting ions on the adsorption capacity of the CS-U membrane, the common anions in Cr(vi)-containing wastewater, such as Cl^- , SO_4^{2-} , and NO_3^- , and the common cations, such as Cu^{2+} , Zn^{2+} , and Ni^{2+} , were added into the $\text{K}_2\text{Cr}_2\text{O}_7$ solution for the batch adsorption experiments. The concentration of each coexisting ion was the same as Cr(vi), which was $\text{50 mg} \cdot \text{L}^{-1}$.

As shown in Figure 8, the adsorption of Cr(vi) by the CS-U membrane was affected by three anions in the order of ${\rm SO_4}^{2^-} > {\rm Cl}^- > {\rm NO_3}^-$. The presence of ${\rm SO_4}^{2^-}$ decreased the adsorption capacity by 57.9%, mainly due to the strong affinity between ${\rm SO_4}^{2^-}$ and protonated amine groups (37,38). The strong competition for adsorption sites led to the

significant reduction of Cr(vi) removal. In contrast, the presence of Cl⁻ and NO₃⁻ had no significant adverse effect on the adsorption capacity of CS-U, with both adsorption capacity reductions within 5%. As for the three metal ions, the order of their influence on the adsorption was Cu²⁺ > $Ni^{2+} > Zn^{2+}$. Although the amine groups on CS had some chelating effect on divalent metal ions (39,40), the electrostatic repulsion between the protonated amine groups and the metal ions exceeded the chelating effect, and thus, the presence of all three metal ions had a minor effect on the adsorption capacity of the CS-U membrane. Even Cu²⁺, which had the greatest effect, only decreased the adsorption capacity by about 10%. In summary, the CS-U membrane can adsorb Cr(vi) substantially in a complex environment where a variety of ions coexist, only SO_4^{2-} will have a noticeable negative effect on the adsorption.

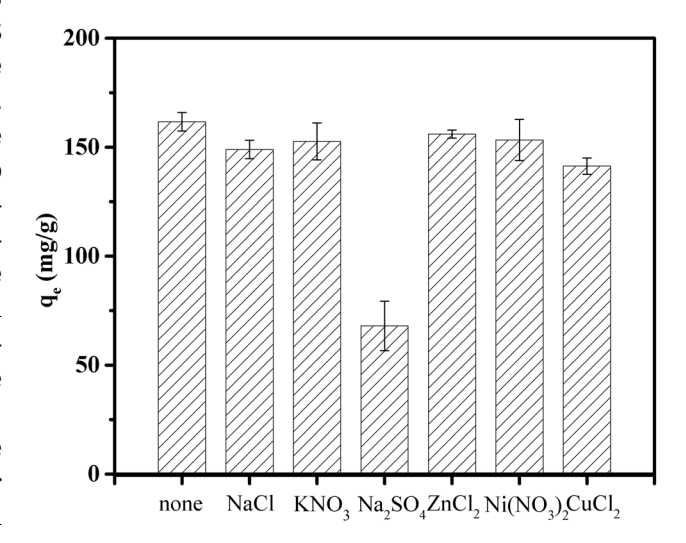


Figure 8: Effect of coexisting ions on the adsorption capacity of the CS-U membrane (experimental conditions: m = 10 mg, $C_0 = 50 \text{ mg} \cdot \text{L}^{-1}$, V = 50 mL, $T = 25^{\circ}\text{C}$, pH = 3).

3.3.5 Selective adsorption and chromium recovery

DE GRUYTER

Although Cr(vi) in wastewater is a hazardous pollutant, chromium is an essential raw material for the metallurgical and chemical industries. If the CS-U membrane can selectively adsorb Cr(vi) in industrial wastewater where multiple metal ions coexist, it will have a positive significance for the recycling of metal resources. In this experiment, 10 mg of the CS-U membrane was added to 50 mL of mixed simulated wastewater containing Cr₂O₇²⁻, Cu²⁺, Zn²⁺, and Ni²⁺ with a concentration of 50 mg·L⁻¹ for each metal ion. The adsorption amounts of the four metal ions by the CS-U membrane were determined by ICP-OES, and the experimental results are shown in Table 4. As can be seen from the table, the CS-U membrane adsorbed Cr(vI), Cu²⁺, and a small amount of Ni²⁺ in the weakly acidic solutions at pH = 4 and 5. In contrast, the CS-U membrane exhibited highly selective adsorption by only adsorbing Cr(vi) under strongly acidic conditions at pH = 2 and 3.

Prolonged immersion in the highly acidic and oxidizing Cr(vi) solution caused irreversible damage to the CS-U membrane, which led to the poor reusability of the membrane. During the adsorption process, the color of the membrane changed from light gray to dark brown, and the nanofibers swelled and eventually disappeared. However, the high adsorption capacity and selectivity of the CS-U membrane for Cr(v1) in strongly acidic environment are very favorable to the recovery of chromium. Based on the results of selective adsorption experiments, the Cr(vi)loaded CS-U membrane was placed in a muffle furnace and heated to 700°C under air atmosphere for 2 h. The ash obtained was a dark green powder, which was thereafter analyzed using an X-ray diffractometer (Ultima III, Rigaku, Japan). The XRD spectrum in Figure 9 showed that the ash was Cr₂O₃ and almost free of other metal oxides. In selective adsorption experiments, approximately 195 mg of Cr₂O₃ can be recovered from 1g of CS-U membrane. For pure K₂Cr₂O₇ solution at pH = 3, 1g of CS-U membrane can theoretically recover a maximum of 310 mg of Cr₂O₃. It is worth mentioning that the adsorption capacity and selectivity of the CS-U

Table 4: Selective adsorption of various metal ions by the CS-U membrane at different pHs

Solution pH	q_e (mg·g $^{-1}$)			
	Cr(vɪ)	Cu(II)	Ni(II)	Zn(II)
5	101.3	50.8	0.5	0
4	104.7	36.9	0	0
3	133.3	0	0	0
2	119.3	0	0	0

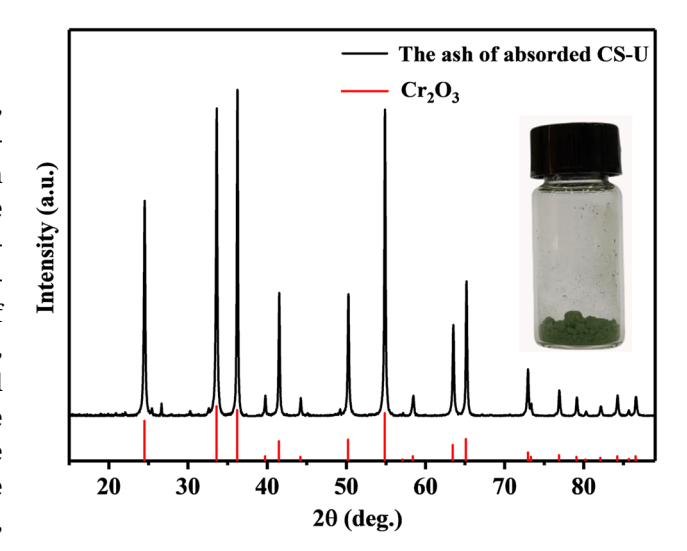


Figure 9: XRD spectra of the ash obtained from the Cr(vI)-loaded CS-U membrane.

membrane for Cr(vi) could be maximized simultaneously by adjusting the pH of the wastewater, which provided very favorable conditions for the recovery of high-purity Cr₂O₃.

3.4 Continuous adsorption

The continuous adsorption experiments help to evaluate the potential application prospects of an adsorbent, and the experimental results are instructive for the design of fixed-bed adsorption plants. In the continuous adsorption experiments, the CS-U membrane was loaded into a 2 cm diameter adsorption column. The K₂Cr₂O₇ solution (10 mg·L⁻¹,

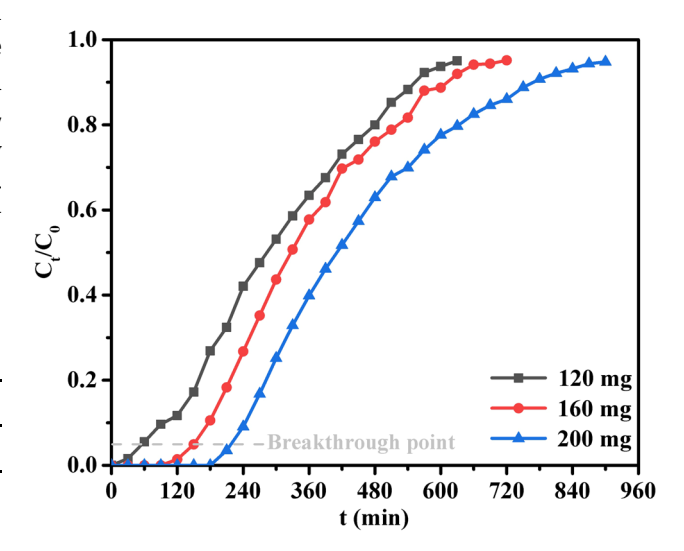


Figure 10: Breakthrough curves of the continuous adsorption of Cr(vI) by the CS-U membrane.

pH = 3) was pumped in from the bottom of the column at a flow rate of 4 mL·min⁻¹ using a peristaltic pump, and the effluent flowed out from the top of the column. It can be seen from the breakthrough curves in Figure 10 that the times of breakthrough were 60, 150, and 210 min for membrane doses of 120, 160, and 200 mg, respectively. According to China's national standard GB8978-2002, industrial wastewater should be discharged with a Cr(vi) concentration of less than 0.5 mg·L⁻¹, which means that 0.2 g of the CS-U membrane is sufficient to treat more than 840 mL of simulated wastewater to meet the discharge standard. In the batch experiments, the adsorption capacity of the CS-U membrane was 74.74 mg·g⁻¹ when the initial Cr(vi) concentration was 10 mg·L⁻¹. In continuous adsorption mode, the saturated adsorption capacity q_{exh} reached 95.21–106.16 mg·g⁻¹ at exhaustion, which was significantly higher than that of static adsorption at the same concentration, effectively verifying the potential of the CS-U membrane for practical application.

China (2023J011393, 2022J05231, and 2021J011021), Foreign Cooperation Project of Fujian Province (2023I0037), and Fuzhou Science and Technology Bureau (2022-Y-005).

Author contributions: Xiaoyu Jie: investigation, methodology, data curation, writing – original draft. Bing-Chiuan Shiu: investigation, formal analysis, visualization. Huazhong Wu: investigation, conceptualization. Yuchi Zhang: data curation, writing – review and editing. Yuansong Ye: resources, funding acquisition. Chunxiang Lin: conceptualization, methodology, validation, funding acquisition. Run Fang: conceptualization, methodology, supervision, funding acquisition, writing – review and editing.

Conflict of interest: The authors state no conflict of interest.

Data availability statement: The data are available from the corresponding author on reasonable request.

4 Conclusion

A novel environmentally friendly nanofiber membrane adsorbent was prepared by electrospinning CS using urushiol as the cross-linking agent. The addition of urushiol not only transformed the linear CS molecules into a stable cross-linked network, but also endowed the composite membrane with a certain degree of hydrophobicity and reducibility. Compared with the CS nanofiber membrane cross-linked with C5H8O2, the CS-U membrane exhibited stronger acid resistance and reducibility, which enabled it to adsorb Cr(vi) effectively from wastewater in a strongly acidic environment. The maximum adsorption capacity reached 204.50 mg·g⁻¹ at 25°C. Benefited from the nanoscale fibers and porous structure, the adsorption rate of the CS-U membrane is much higher than that of conventional bulk or granular CS-based adsorbents. The adsorption amount reached 72.89 and 142.01 mg·g⁻¹ after 30 min and 2 h adsorption, respectively. Due to the highly selective adsorption of Cr(vi) in acidic environments, high purity Cr₂O₃ was recovered by ashing the adsorbed CS-U membrane in a muffle furnace. In addition to batch adsorption, the CS-U membrane also performed well in continuous adsorption mode. Only 0.2 g of the CS-U membrane was sufficient to treat more than 840 mL of Cr(vi)-containing wastewater with a concentration of 10 mg·L⁻¹ to meet the discharge standard of less than 0.5 mg·L⁻¹, verifying the potential of the CS-U membrane for practical application.

Funding information: This work was financially supported by the Natural Science Foundation of Fujian Province of

References

- Saha R, Nandi R, Saha B. Sources and toxicity of hexavalent chromium. J Coord Chem. 2011;64(10):1782–806. doi: 10.1080/00958972. 2011.583646.
- (2) Dayan AD, Paine AJ. Mechanisms of chromium toxicity, carcinogenicity and allergenicity: Review of the literature from 1985 to 2000. Hum Exp Toxicol. 2001;20:439–51. doi: 10.1191/096032701682693062.
- (3) Costa M, Klein CB. Toxicity and carcinogenicity of chromium compounds in humans. Crit Rev Toxicol. 2006;36(2):155–63. doi: 10. 1080/10408440500534032.
- (4) Kongsricharoem N, Polprasert C. Chromium removal by a bipolar electro-chemical precipitation process. Water Sci Technol. 1996;34(9):109–16. doi: 10.1016/s0273-1223(96)00793-7.
- (5) Peng H, Guo J. Removal of chromium from wastewater by membrane filtration, chemical precipitation, ion exchange, adsorption electrocoagulation, electrochemical reduction, electrodialysis, electrodeionization, photocatalysis and nanotechnology: a review. Environ Chem Lett. 2020;18:2055–68. doi: 10.1007/s10311-020-01058-x
- Rengaraj S, Yeon KH, Moon SH. Removal of chromium from water and wastewater by ion exchange resins. J Hazard Mater. 2001;87(1–3):273–87. doi: 10.1016/s0304-3894(01)00291-6.
- (7) Wang HM, Song XY, Zhang HH, Tan P, Kong FX. Removal of hexavalent chromium in dual-chamber microbial fuel cells separated by different ion exchange membranes. J Hazard Mater. 2020;384:121459. doi: 10.1016/j.jhazmat.2019.121459.
- (8) Kononova ON, Bryuzgina GL, Apchitaeva OV, Kononov YS. Ion exchange recovery of chromium (vi) and manganese (II) from aqueous solutions. Arab J Chem. 2019;12(8):2713–20. doi: 10.1016/j. arabjc.2015.05.021.
- (9) He PY, Zhang YJ, Chen H, Han ZC, Liu LC. Low-cost and facile synthesis of geopolymer-zeolite composite membrane for chromium(vi) separation from aqueous solution. J Hazard Mater. 2020;392:122359. doi: 10.1016/j.jhazmat.2020.122359.

- (10) Kozlowski CA, Walkowiak W. Removal of chromium(v₁) from aqueous solutions by polymer inclusion membranes. Water Res. 2002;36(19):4870–6. doi: 10.1016/S0043-1354(02)00216-6.
- (11) Geng JJ, Yin YW, Liang QW, Zhu ZJ, Luo HJ. Polyethyleneimine cross-linked graphene oxide for removing hazardous hexavalent chromium: Adsorption performance and mechanism. Chem Eng J. 2019;361:1497–510. doi: 10.1016/j.cej.2018.10.141.
- (12) Dognani G, Hadi P, Ma HY, Cabrera FC, Job AE, Agostini DS, et al. Effective chromium removal from water by polyaniline-coated electrospun adsorbent membrane. Chem Eng J. 2019;372:341–51. doi: 10.1016/j.cej.2019.04.154.
- (13) Hu XJ, Wang JS, Liu YG, Li X, Zeng GM, Bao ZL, et al. Adsorption of chromium (vi) by ethylenediamine-modified cross-linked magnetic chitosan resin: Isotherms, kinetics and thermodynamics. . J Hazard Mater. 2011;185(1):306–14. doi: 10.1016/j.jhazmat.2010.09.034.
- (14) Gokila S, Gomathi T, Sudha PN, Anil S. Removal of the heavy metal ion chromiuim(vi) using Chitosan and Alginate nanocomposites. Int J Biol Macromol. 2017;104:1459–68. doi: 10.1016/j.ijbiomac.2017.05.117.
- (15) Beppu MM, Vieira RS, Aimoli CG, Santana CC. Crosslinking of chitosan membranes using glutaraldehyde: Effect on ion permeability and water absorption. J Membrane Sci. 2007;301(1–2):126–30. doi: 10.1016/j.memsci.2007.06.015.
- (16) Chiou MS, Li HY. Adsorption behavior of reactive dye in aqueous solution on chemical cross-linked chitosan beads. Chemosphere. 2003;50(8):1095–105. doi: 10.1016/s0045-6535(02)00636-7.
- (17) Chen AH, Liu SC, Chen CY, Chen CY. Comparative adsorption of Cu (II), Zn(II), and Pb(II) ions in aqueous solution on the crosslinked chitosan with epichlorohydrin. J Hazard Mater. 2008;154(1–3):184–91. doi: 10.1016/j.jhazmat.2007.10.009.
- (18) Jeong S, Kim D, Seo J. Preparation and antimicrobial properties of LDPE composite films melt-blended with polymerized urushiol powders (YPUOH) for packaging applications. Prog Org Coat. 2015;85:76–83. doi: 10.1016/j.porgcoat.2015.03.012.
- (19) Bai WB, Chen KH, Chen JP, Xu J, Lin HM, Lin YC, et al. Natural Highly-hydrophobic urushiol@TiO₂ coated cotton fabric for effective oil-water separation in highly acidic alkaline and salty environment. Sep Purif Technol. 2020;253:117495. doi: 10.1016/j.seppur.2020.117495.
- (20) Su YN, Zheng XL, Cheng HY, Rao MH, Chen KD, Xia JR, et al. Mn-Fe₃O₄ nanoparticles anchored on the urushiol functionalized 3D-graphene for the electrochemical detection of 4-nitrophenol. J Hazard Mater. 2021;409:124926. doi: 10.1016/j.jhazmat.2020.124926.
- (21) Watanabe H, Fujimoto A, Takahara A. Characterization of catecholcontaining natural thermosetting polymer "urushiol" thin film. J Polym Sci Pol Chem. 2013;51(17):3688–92. doi: 10.1002/pola.26770.
- (22) Jie XY, Shiu BC, Zhang YC, Wu HZ, Ye YS, Fang R. Chitosan-Urushiol nanofiber membrane with enhanced acid resistance and broad-spectrum antibacterial activity. Carbohydr Polym. 2023;312:120792. doi: 10.1016/j.carbpol.2023.120792.
- (23) Samuel MS, Bhattacharya J, Raj S, Santhanam N, Singh H, Pradeep SD. Efficient removal of Chromium(vi) from aqueous solution using chitosan grafted graphene oxide (CS-GO) nanocomposite. Int J Biol Macromol. 2019;121:285–92. doi: 10.1016/j. iibiomac.2018.09.170.
- (24) Li L, Li YX, Cao LX, Yang CF. Enhanced chromium (vi) adsorption using nanosized chitosan fibers tailored by electrospinning. Carbohydr Polym. 2015;125:206–13. doi: 10.1016/j.carbpol.2015.02.037.
- (25) Zhang L, Wu HT, Zheng ZY, He HC, Wei M, Huang XH. Fabrication of graphene oxide/multi-walled carbon nanotube/urushiol formaldehyde polymer composite coatings and evaluation of their

- physico-mechanical properties and corrosion resistance. Prog Org Coat. 2019;127:131–9. doi: 10.1016/j.porgcoat.2018.10.026.
- (26) Watanabe H, Fujimoto A, Nishida J, Ohishi T, Takahara A. Biobased Polymer coating using catechol derivative urushiol. Langmuir. 2016;32(18):4619–23. doi: 10.1021/acs.langmuir.6b00484.
- (27) Gan C, Liu YG, Tan XF, Wang SF, Zeng GM, Zheng BH, et al. Effect of porous zinc–biochar nanocomposites on Cr(vi) adsorption from aqueous solution. RSC Adv. 2015:5:35107–15. doi: 10.1039/c5ra04416b.
- (28) Huang XX, Liu YG, Liu SB, Tan XF, Ding Y, Zeng GM, et al. Effective removal of Cr(vi) using β-cyclodextrin–chitosan modified biochars with adsorption/reduction bifuctional roles. RSC Adv. 2016;6:94–104. doi: 10.1039/c5ra22886g.
- (29) Mohan D, Pittman Jr CU. Activated carbons and low cost adsorbents for remediation of tri- and hexavalent chromium from water. J Hazard Mater. 2006;137(2):762–811. doi: 10.1016/j.jhazmat.2006. 06.060.
- (30) Zhang H, Peng L, Chen AW, Shang C, Lei M, He K, et al. Chitosanstabilized FeS magnetic composites for chromium removal: Characterization, performance, mechanism, and stability. Carbohydr Polym. 2019;214:276–85. doi: 10.1016/j.carbpol.2019.03.056.
- (31) Niu CW, Zhang N, Hu CC, Zhang CY, Zhang HH, Xing YJ. Preparation of a novel citric acid-crosslinked Zn-MOF/chitosan composite and application in adsorption of chromium(vi) and methyl orange from aqueous solution. Carbohydr Polym. 2021;258:117644. doi: 10.1016/ j.carbpol.2021.117644.
- (32) Boddu VM, Abburi K, Talbott JL, Smith ED. Removal of hexavalent chromium from wastewater using a new composite chitosan biosorbent. Environ Sci Technol. 2003;37(19):4449–56. doi: 10.1021/ es021013a.
- (33) Li ZY, Li TT, An LB, Fu PF, Gao CJ, Zhang ZM. Highly efficient chromium(VI) adsorption with nanofibrous filter paper prepared through electrospinning chitosan/polymethylmethacrylate composite. Carbohydr Polym. 2016;137:119–26. doi: 10.1016/j.carbpol. 2015.10.059.
- (34) Vilela PB, Dalalibera A, Duminelli EC, Becegato VA, Paulino AT. Adsorption and removal of chromium (vi) contained in aqueous solutions using a chitosan-based hydrogel. Environ Sci Pollut Res. 2019;26:28481–9. doi: 10.1007/s11356-018-3208-3.
- (35) Li LL, Fan LL, Sun M, Qiu HM, Li XJ, Duan HM, et al. Adsorbent for chromium removal based on graphene oxide functionalized with magnetic cyclodextrin-chitosan. Colloid Surface B. 2013;107:76–83. doi: 10.1016/j.colsurfb.2013.01.074.
- (36) Rahmani O, Bouzid B, Guibadj A. Extraction and characterization of chitin and chitosan: applications of chitosan nanoparticles in the adsorption of copper in an aqueous environment. e-Polymers. 2017;17(5):383–97. doi: 10.1515/epoly-2016-0318.
- (37) Shekhawat A, Kahu S, Saravanan D, Jugade R. Synergistic behaviour of ionic liquid impregnated sulphate-crosslinked chitosan towards adsorption of Cr(vi). Int J Biol Macromol. 2015;80:615–26. doi: 10. 1016/j.ijbiomac.2015.07.035.
- (38) Kahu S, Saravanan D, Jugade R. Effective detoxification of hexavalent chromium using sulfate-crosslinked chitosan. Water Sci Technol. 2014;70(12):2047–55. doi: 10.2166/wst.2014.455.
- (39) Chen J, Zhao K, Liu L, Gao YY, Zheng L, Liu M. Modified kaolin hydrogel for Cu²⁺ adsorption. e-Polymers. 2022;22(1):986–96. doi: 10.1515/epoly-2022-0085.
- (40) Zhu YH, Hu J, Wang JL. Competitive adsorption of Pb(II), Cu(II) and Zn(II) onto xanthate-modified magnetic chitosan. J Hazard Mater. 2012;221–222:155–61. doi: 10.1016/j.jhazmat.2012.04.026.